Expansion of distinct peripheral blood myeloid cell subpopulations in patients with rheumatoid arthritis-associated interstitial lung disease

Jill A. Poole [a,*], Kathryn E. Cole [b], Geoffrey M. Thiele [a], James E. Talmadge [a,b], Bryant R. England [a,c], Amy J. Nelson [a], Angela Gleason [a], Aaron Schwab [a], Rohit Gaurav [a], Michael J. Duryee [a,c], Kristina L. Bailey [a,c], Debra J. Romberger [a,c], Daniel Hershberger [a], Joel Van De Graaff [a,c], Sara M. May [a,c], Rhonda Walenz [a], Bridget Kramer [a], Ted R. Mikuls [a,c]

[a] *Department of Internal Medicine, USA*
[b] *Department of Pathology and Microbiology, College of Medicine, University of Nebraska Medical Center, Omaha, NE, USA*
[c] *Veterans Affairs Nebraska-Western Iowa Health Care System, Omaha, NE, USA*

ARTICLE INFO

ABSTRACT

Objectives: Interstitial lung disease (ILD) is associated with significant mortality in rheumatoid arthritis (RA) patients with key cellular players remaining largely unknown. This study aimed to characterize inflammatory and myeloid derived suppressor cell (MDSC) subpopulations in RA-ILD as compared to RA, idiopathic pulmonary fibrosis (IPF) without autoimmunity, and controls.

Methods: Peripheral blood was collected from patients with RA, RA-ILD, IPF, and controls (N = 60, 15/cohort). Myeloid cell subpopulations were identified phenotypically by flow cytometry using the following markers: CD45,CD3,CD19,CD56,CD11b,HLA-DR,CD14,CD16,CD15,CD125,CD33. Functionality of subsets were identified with intracellular arginase-1 (Arg-1) and inducible nitric oxide synthase (iNOS) expression.

Results: There was increased intermediate (CD14^{++}CD16^{+}) and nonclassical (CD14$^{+/-}$CD16^{++}) and decreased classical (CD14^{++}CD16^{-}) monocytes in RA, RA-ILD, and IPF vs. control. Intermediate monocytes were higher and classical monocytes were lower in RA-ILD vs. RA but not IPF. Monocytic (m)MDSCs were higher in RA-ILD vs. control and RA but not IPF. Granulocytic (g)MDSCs did not significantly differ. In contrast, neutrophils were increased in IPF and RA-ILD patients with elevated expression of Arg-1 sharing similar dimensional clustering pattern. Eosinophils were increased in RA-ILD vs. controls, RA and IPF. Across cohorts, iNOS was decreased in intermediate/nonclassical monocytes but increased in mMDSCs vs. classical monocytes. In RA-ILD, iNOS positive mMDSCs were increased versus classic monocytes.

Conclusions: Myeloid cell subpopulations are significantly modulated in RA-ILD patients with expansion of CD16^{+} monocytes, mMDSCs, and neutrophils, a phenotypic profile more aligned with IPF than other RA patients. Eosinophil expansion was unique to RA-ILD, potentially facilitating disease pathogenesis and providing a future therapeutic target.

1. Introduction

Interstitial lung disease (ILD) is associated with significant morbidity and mortality in rheumatoid arthritis (RA), clinically impacting up to 10 % of patients with RA and subclinically affecting up to 40 % [1,2]. There are several patterns of ILD demonstrated in RA including usual interstitial pneumonia (UIP), nonspecific interstitial pneumonia, obliterative bronchiolitis, and organizing pneumonia with collective computed tomography imaging features of subpleural, basal predominant, reticular abnormalities with honeycombing, bronchiectasis, and ground-glass opacities [3]. In comparison, idiopathic pulmonary fibrosis (IPF) is characterized by UIP findings in the absence of autoimmunity. Although there have been improvements in therapeutic approaches for ILD and the associated pulmonary fibrosis, including the availability of anti-fibrotic therapies, these therapies have limited efficacy [4,5], and respiratory disease remains a frequent cause of death in RA [6,7]. The pathogenesis of RA-ILD is complex and current considerations in its pathogenesis include autoimmunity, dysregulation of inflammatory and

fibrotic pathways, oxidative stress, and exposure to various environmental/occupational factors in genetically susceptible individuals [6,8]. In addition, the critical cellular mediators of RA-ILD remain largely unknown. Whereas early studies supported generalized roles for neutrophils, macrophages, and lymphocytes in RA-associated lung disease [9], the complexity and spectrum of cellular phenotypes is increasingly appreciated in lung inflammatory-fibrosis processes [10].

Although there are increasingly recognized roles of myeloid cell subpopulations in RA and idiopathic (non-autoimmune) pulmonary fibrosis (IPF) pathophysiology, in contrast little is known about their contributions in RA-ILD. Myeloid cells including granulocytes (e.g., neutrophils and eosinophils), monocytic cells, and subpopulations of myeloid derived suppressor cells (MDSCs) are considered to have roles in these pathologies. Peripheral blood HLA-DR$^+$ monocytes are classified by expression of CD14 and CD16 into the major subpopulation of classical monocytes (CD14^{++}CD16$^-$) and minor subpopulations of intermediate (CD14^{++}CD16$^+$) and nonclassical (CD14$^{+/-}$CD16^{++}) monocytes [11]. Intermediate and nonclassical (CD16$^+$) monocytes are associated with several inflammatory diseases including early RA and particularly RA characterized by active joint disease [12–14]. In both IPF and RA-ILD, high monocyte counts are associated with poor prognosis [15–17] and targeting these cells reduces disease progression in a mouse model of bleomycin-induced pulmonary fibrosis [18].

MDSCs are a heterogeneous population of immature myeloid cells with suppressor capabilities, typically delineated as granulocytic (g) MDSCs and monocytic (m)MDSCs and are associated with poor prognosis in cancer [19]. There is limited evidence suggesting a potential association of mMDSCs and gMDSCs in inflammatory diseases including RA and IPF in humans (and mice), although results from these studies are conflicting [20–22]. Eosinophils, are generally regarded as end-stage effector cells, but have gained a recognized role across disease states due to their immunoregulatory roles [23] as well as the expansion of approved eosinophil-targeted therapies in obstructive lung diseases [24,25]. The function of myeloid cells can be assessed by assessing Arg-1 and inducible nitrous oxide synthase (iNOS), expression correlated to both effector and suppressive cell features [20,26–28]. However, few studies have characterized all these myeloid cell subpopulations within autoimmune subjects and across the disease entities.

The objective of this study was to rigorously characterize peripheral blood myeloid cell subpopulations including monocytes, neutrophils, eosinophils, and MDSCs collectively in RA-ILD patients in comparison to patients with RA without lung disease and patients with IPF without autoimmunity with a comparator control group to gain insight into underlying disease pathogenesis and to identify future therapeutic targets for RA-ILD.

2. Patients and methods

2.1. Peripheral blood samples

Blood samples from participants were obtained after receiving written informed consent and following approval of the Institutional Review Board at the Veterans Affairs (VA) Nebraska-Western Iowa Health Care System and University of Nebraska Medical Center (UNMC). Blood was collected between January 2022 and January 2023. All patients with RA fulfilled the 1987 American College Rheumatology classification criteria [29]. The presence of RA-ILD was confirmed by a board-certified subspecialist (pulmonologist or rheumatologist) and the presence of supportive chest computed tomography (CT) findings. RA-ILD was further categorized based on chest CT findings in the clinical radiology reports as those with: 1) usual interstitial pneumonia (UIP), honeycombing or fibrosis, 2) ground glass opacities [30], or 3) other/indeterminate (e.g., subpleural reticulation, interstitial thickening, or reticular opacities), based on prior work [31]. Patients were defined as having RA without ILD in the absence of a clinical diagnosis of ILD or past chest imaging findings suggestive of ILD. All patients with IPF

without underlying autoimmune disease were diagnosed by a board-certified pulmonologist and had confirmatory findings of UIP by chest CT imaging. A convenience sample of "control" comparator patients were all recruited from the VA allergy clinic and included patients with allergic rhinitis on specific allergy desensitization and in the absence of clinically apparent lung disease and/or autoimmunity. Venous blood samples were collected in EDTA tubes and processed within 2 h of collection.

2.2. Dyspnea symptom assessment and clinical data

Participants completed the University of California, San Diego (UCSD) Shortness of Breath Questionnaire (SOBQ), a 24-item dyspnea questionnaire with score ranges of 0 to 120, with higher scores indicating greater dyspnea [32]. For patients with RA, clinical data, disease severity, and medication use were recorded by treating rheumatologists and lung function indices for IPF were abstracted from patients' medical records.

2.3. Multicolor staining and acquisition

Membrane immunophenotypic staining was conducted on all fresh blood samples (1.5 mL per participant) following lysis of red blood cells (RBC) with RBC lysis buffer (NH$_4$CL-NaHCO$_3$- EDTA). Post lysis, cells were washed and neutralized in flow cytometry staining (FACS) buffer (2 % Fetal Bovine Serum and 0.1 % sodium azide in phosphate buffered saline (PBS)) prior to enumeration using a BioRad TC 20 cell counter. Cells were aliquoted at 5x10^5 cells/ml/tube for all samples. Cells were incubated with LIVE/DEAD Fixable Blue Dead Cell Stain Kit (Invitrogen, Carlsbad, CA) and CD16/32 (Fc Block, Biolegend, San Diego, CA) to minimize non-specific antibody staining. Cells were stained with monoclonal antibody against mouse anti-human CD45 (clone:2D1), CD16 (clone:3G8), CD15 (clone:W6D3), CD14 (clone:63D3), CD11b (clone:M1/70), CD33 (clone:P67.6)(Biolegend); CD125 (clone:A14), CD3 (clone:UCHT1), CD19 (clone:SJ25C1), CD56 (clone:NCAM16.2) (BD Biosciences, Franklin Lakes, NJ); and anti-HLA-DR (clone:L203) (R&D Systems, Minneapolis, MN).

2.4. Functional assessments of intracellular iNOS and Arg-1 by myeloid subsets

To functionally assess myeloid subpopulations, cells were also stained for expression of intracellular iNOS and Arg-1 [20,26–28]. Expression of iNOS and Arg-1 has been directly correlated to T-cell suppression as well as decreases in T cell activation, proliferation, and signaling [20,26–28]. The FIX & PERM Cell Permeabilization Kit (Invitrogen) was utilized for intracellular staining of enzyme targets using anti-Arg-1 (polyclonal antibody:NBP1-32731G) and anti-iNOS (clone:4Es, NBP2-22119FR)(Novus, Centennial, CO).

Cells were acquired the same day on a BD LSRII Yellow/Green cytometer configured with 355-nm, 405-nm, 488-nm, 561-nm, and 633-nm lasers.

2.5. Cytometric data analysis

Post-acquisition, data were exported and stored using the flow cytometry standard (FCS) 3.1 format and analyzed using FlowJo software version 10.8 (FlowJo, Ashland, OR). Fluorescence was compensated using all single-stained compensation tubes. Fluorescence Minus One (FMO) controls were used to set the upper boundary for background signal. The gating strategy was modeled from previous work from members of our research team [33]. All panels were first gated as forward scatter-area (FSC-A) x side scatter-area (SSC-A) to omit debris, dead, or apoptotic cells. Next, two single-cell gates to omit doublets (FSC-A x FSC height (H) and SSC-A x SSC-H), followed by a live/dead gate and then a CD45 gate. CD45$^+$ cells were placed on a lineage (LIN)

gate to record LIN⁺ lymphocytes (CD3⁺ T cells, CD19⁺ B cells, and CD56⁺ natural killer (NK) cells) and select LIN⁻ cells (remove lymphocytes). A CD11b⁺ gate was applied to LIN⁻ cells to collect CD11b⁺ myeloid cells. This gating strategy is depicted in Supplemental Figure 1.

CD11b⁺ cells were then gated on HLA-DR x SSC-A to collect HLA-DR^{hi}SSC^{lo} monocytes. The HLA-DR^{hi}SSC^{lo} gated cells were then gated against CD15 to remove any remaining granulocytes. This CD11b⁺HLA-DR^{hi}SSC^{lo} population was then gated on CD14 and CD16 expression to delineate classical monocytes (CD14^{++}CD16⁻), intermediate monocytes (CD14^{++}CD16⁺), and non-classical monocytes (CD14$^{+/-}$CD16^{++}). The CD11b⁺HLA-DR^{lo} cells were gated on CD15 to collect either CD16^{hi} cells or CD16^{lo} cells. CD16^{hi} cells were gated on CD15 to confirm HLA-DR^{lo}CD11b⁺CD16⁺CD15⁺ neutrophils. The CD16^{lo} population was gated on a CD15 x CD14 gate followed by CD125 (IL-5Rα) x CD33 or CD33 x SSC-A to collect monocytic (m)MDSCs (LIN⁻CD11b⁺HLA-DR^{lo}CD14⁺CD16^{lo}CD15^{lo}CD33⁺), immature (i)MDSCs (LIN⁻CD11b⁺HLA-DR^{lo}CD14⁻CD16^{lo}CD15⁻CD33⁺), eosinophils (LIN⁻CD11b⁺HLA-DR^{lo}CD16^{lo}CD15⁺CD125⁺CD33⁻), eosinophilic (Eo)-granulocytic (g)MDSCs (LIN⁻CD11b⁺HLA-DR^{lo}CD16^{lo}CD15⁺CD125⁺CD33⁻), CD33^{dim}CD125⁻ gMDSCs (LIN⁻CD11b⁺HLA-DR^{lo}CD16^{lo}CD15⁺CD125⁻CD33^{dim}), and CD33⁻CD125⁻ gMDSCs (LIN⁻CD11b⁺HLA-DR^{lo}CD16^{lo}CD15⁺CD125⁻CD33⁻). Arg-1 and iNOS are expressed as mean fluorescence intensity [34] or percent positive expression on cell subpopulations. Arg-1 MFI expression on granulocytes reflects subtraction of background staining of subject-matched classical monocyte as controversy exists regarding Arg-1 presence in monocytes [35]. The percentage of respective cell subpopulations were determined from live CD45⁺ leukocytes and cell numbers determined from multiplying this percentage by total leukocytes.

2.6. Clustering, t-distributed stochastic neighbor embedding (tSNE)

We utilized tSNE as an unsupervised nonlinear dimensionality reduction algorithm to visualize the high dimensional flow cytometry data [36]. The FlowJo tSNE platform computes clustering of data from user defined selection of cytometric parameters [36]. To reduce noise in the analysis, non-debris, singlet, live CD45⁺ cell populations from a representative sample from each participant group at 50,000 events/sample were concatenated into one file and analyzed by tSNE with selection of cytometric parameters including FSC-A and SSC-A and uncompensated LIN, CD11b, HLA-DR, CD14, CD15, CD16, CD33, CD125, Arg-1, and iNOS with the following technical options: iterations:1000, perplexity:20, learning rate:14,000, k-nearest neighbors (KNN) algorithm:Exact-vantage point tree, and gradient algorithm:Barnes-Hut. After computation, the embedded tSNE mapping of the combined 4 subjects is shown by contour plotting of tSNE_1 vs. tSNE_2 with overlay labeling based upon aforementioned gating strategies. The 4 representative group samples were then separated for visualization of differences.

2.7. Statistics

A sample size determination was based upon pilot study good practices recommending N = 12/group [37] with additional consideration given for potential technical and/or sample issues (~20 %) to arrive at an a priori sample size determination of N = 15/group (N = 60 total). The actual power achieved (post-hoc power analysis) using continuous endpoint, two-independent sample study (control vs. RA-ILD) was 100 % for classical monocytes, 99.4 % for intermediate monocytes, 39.3 % for nonclassical monocytes, 96.3 % for mMDSCs, 68.3 % for neutrophils and 100 % for eosinophils. Numbers less than 15 per group reflect limitations in staining quality or missing data. One RA-ILD patient was noted to have profound neutropenia (~2%) after enrollment and was excluded in the neutrophil analyses but included for other analyses as there were otherwise no statistical differences with/without this subject (data not shown). For all continuous data, the Shapiro-Wilk test for

normality was first applied. If normally distributed, the parametric one-way analysis of variance (ANOVA) was applied and if not normally distributed, the non-parametric Kruskal-Wallis test was applied. If p-value was less than 0.05, the Benjamini and Hochberg (BH) test was applied for multiple comparisons to control the false discovery rate to determine differences between groups [38]. A repeated measures (RM) ANOVA followed by post-hoc Tukey's comparisons between groups was utilized to determine differences in iNOS expression across matched subject's monocyte subpopulations. All statistical analyses were performed using the GraphPad Prism software, version 9.5 (GraphPad, San Diego, CA, USA) and statistical significance accepted at $p \leq 0.05$.

3. Results

3.1. Participant characteristics

Participant (60 participants, n = 15/group) characteristics are summarized in Table 1. Patients with RA, RA-ILD, and IPF were older than controls, though age was overlapping among the disease groups. Participants across groups were predominately male and self-reported White race, reflecting characteristics of the larger VA population. The history of ever smoking was numerically most frequent among participants with RA and RA-ILD followed by those with IPF and lowest in controls. Shortness of breath as assessed by the UCSD-SOBQ, although generally low, demonstrated increased symptoms (total score) in patients with RA, RA-ILD, and IPF vs. controls with the highest symptomatic dyspnea observed in those with IPF. Based on CT findings, the number of RA-ILD patients categorized as having UIP/fibrosis was 8 (53.3 %), GGO was 2 (13.3 %), and other/indeterminate was 5 (33.3 %). Further characteristics of patients with RA and RA-ILD are listed in Supplemental Table 1.

Table 1
Participant Characteristics.

	ControlN = 15	RAN = 15	RA-ILDN = 15	IPFN = 15
Age, y, median (range)	48 (40–54)	73 (57–78)	73 (68–79)	74 (69–77)
Race, n (%)				
White	13 (86.7)	13 (86.7)	11 (73.3)	15 (1 0 0)
Black/African American	1 (6.7)	0 (0)	3 (20)	0 (0)
Native American	0 (0)	2 (13.3)	1 (6.7)	0 (0)
Other	1 (6.7)	0 (0)	0 (0)	0 (0)
Sex, n (%)				
Male	10 (66.7)	13 (86.7)	14 (93.3)	14 (93.3)
Female	5 (33.3)	2 (13.3)	1 (6.7)	1 (6.7)
Cigarette Smoking, n (%)				
Never	8 (53.3)	2 (13.3)	4 (26.7)	8 (53.3)
Ever	6 (40)	11 (73.3)	10 (66.7)	7 (46.7)
Current	1 (6.7)	2 (13.3)	1 (6.7)	0 (0)
UCSD SOBQ Total Score, median (quartiles)	4 (0–7)	27 (11–66)	31 (10–42)	38 (23–65)
Lung function, median (quartiles)				
FVC % predicted	–	–	85 (72–100)	63 (49–81)
Lung function, median (quartiles)FVC % predictedDLCO % predicted	–	–	56 (49–71)	42 (33–54)

Values: median (range = quartiles 25th-75th percentile) or n (%).
Abbreviations: UCSD SOBQ: University of California, San Diego Shortness of Breath Questionnaire, FVC: Forced vital capacity, DLCO: Diffusion capacity of the lungs for carbon monoxide.

3.2. Frequency of HLA-DR⁺ monocyte subpopulations

Live CD45$^+$CD11b$^+$HLA-DR^{hi}CD15$^-$ monocytes were immunophenotyped based upon CD14 and CD16 expression to delineate classical (CD14^{++}CD16$^-$), intermediate (CD14^{++}CD16$^+$) and non-classical (CD14$^{+/-}$CD16^{++}) monocytes with representative contour plots shown from a control and RA-ILD participant (Fig. 1**A**). The frequency of total monocytes, as a proportion of CD45$^+$ cells, did not differ across groups (Fig. 1**B**). However, the frequency of the monocyte subpopulations comprising the total monocyte population differed by group. There was a significant decrease in the frequency of classical monocytes in RA (-13 %), RA-ILD (-34 %,), and IPF (-27 %) vs. controls. RA-ILD and IPF patients had a significant decrease in the proportion of classical monocytes vs. RA. In contrast, there were significant increases in the frequency of intermediate and non-classical monocytes in RA (+59 %, and + 70 %, respectively), RA-ILD (+160 % and + 178 %, respectively), and IPF (+110 %, and + 167 %, respectively). As compared to RA but not IPF, there was a significant increase in intermediate monocytes in RA-ILD patients.

### 3.3. Frequency of monocytic (m)MDSCs and immature (i)MDSCs

mMDSCs and iMDSCs were gated separate from HLA-DR^{hi} monocytes with representative gating plots shown for control and RA-ILD participants (Fig. 2**A-B**). There were significant increases in the frequency of mMDSCs, as a proportion of CD45$^+$ cells, with RA (+214 %), RA-ILD (+571 %), and IPF (+286 %) vs. controls with a significant increase in mMDSCs in RA-ILD (but not IPF) vs. RA (+114 %) (Fig. 2**C**).

There was no difference in the frequency of iMDSCs as a proportion of CD45$^+$ cells across groups (Fig. 2**D**).

### 3.4. Frequency of neutrophils, eosinophils, and gMDSCs

Granulocytes (neutrophils, eosinophils, and gMDSCs) were gated separate from monocytes, mMDSCs and iMDSCs with representative gating plots shown for a control and RA-ILD participant (Fig. 2**A-B**). There were significant increases in the frequency of total neutrophils as a proportion of CD45$^+$ cells with IPF (+20 %) and RA-ILD (+14 %, excluding the profound neutropenic outlier) but not with RA vs. controls (Fig. 2**E**). However, the significant increase in frequency of neutrophils is lost when including the outlier (+6.5 %, p = 0.1). This subject was removed from the neutrophil Arg-1 and iNOS analyses.

Eosinophils were gated separately from monocytes, neutrophils, mMDSCs, gMDSDCs, and iMDSCs (Fig. 2**A–B**). There were significant increases in the frequency of eosinophils, as a proportion of CD45$^+$ cells, with RA-ILD (+144 %) but not IPF vs. controls and non-significant trends for RA (+49 %, p = 0.08) vs. controls (Fig. 2**F**). The frequency of eosinophils was also increased in RA-ILD vs. IPF. Finally, gMDSCs were gated from all other populations and subpopulations based upon CD33 and CD125 expression (Fig. 2**A–B**). There was no significant difference in the frequency of Eo-gMDSCs (Fig. 2**G**) or CD33$^-$CD125$^-$ gMDSCs (Fig. 2**I**) across groups. However, there was a significant increase in the frequency of CD125$^-$CD33^{dim} gMDSCs in RA-ILD subjects (+72 %) vs. controls (Fig. 2**H**).
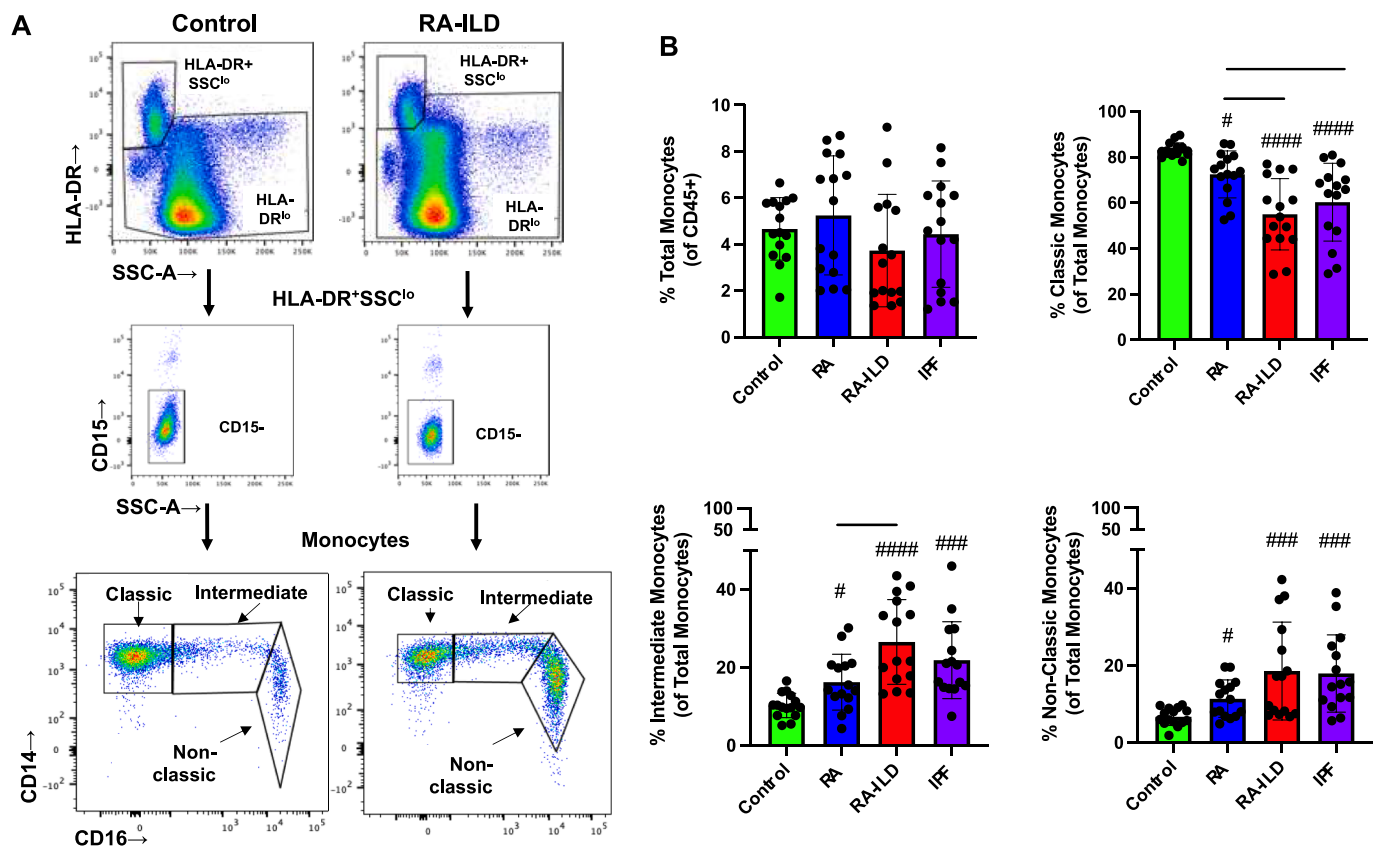
Fig. 1. Peripheral HLA-DR$^+$ blood monocyte subpopulations vary across RA, RA-ILD, and IPF vs. controls. **A**, Representative contour plots depicting gating of classical (CD14^{++}CD16$^-$), intermediate (CD14^{++}CD16$^+$), and non-classical (CD14$^+$CD16^{++}) monocytes with representative plots shown of a control and RA-ILD participant. Top panel shows non-debris, live, singlets, CD45$^+$LIN$^-$CD11b$^+$ cells (*see Supplemental* Figure 1) gated on HLA-DR high vs. low expression and side scatter properties followed by exclusion of CD15$^+$ cells (middle panel) for monocyte subpopulations determination based upon CD14 and CD16 expression (bottom panel). **B**, Scatter plots with bars depict mean with SEM. N = 15 subjects/group. Statistical difference (#p < 0.05, ##p < 0.01, ###p < 0.001, ####p < 0.0001) vs. control and between groups denoted by line (*p < 0.05, **p < 0.01).
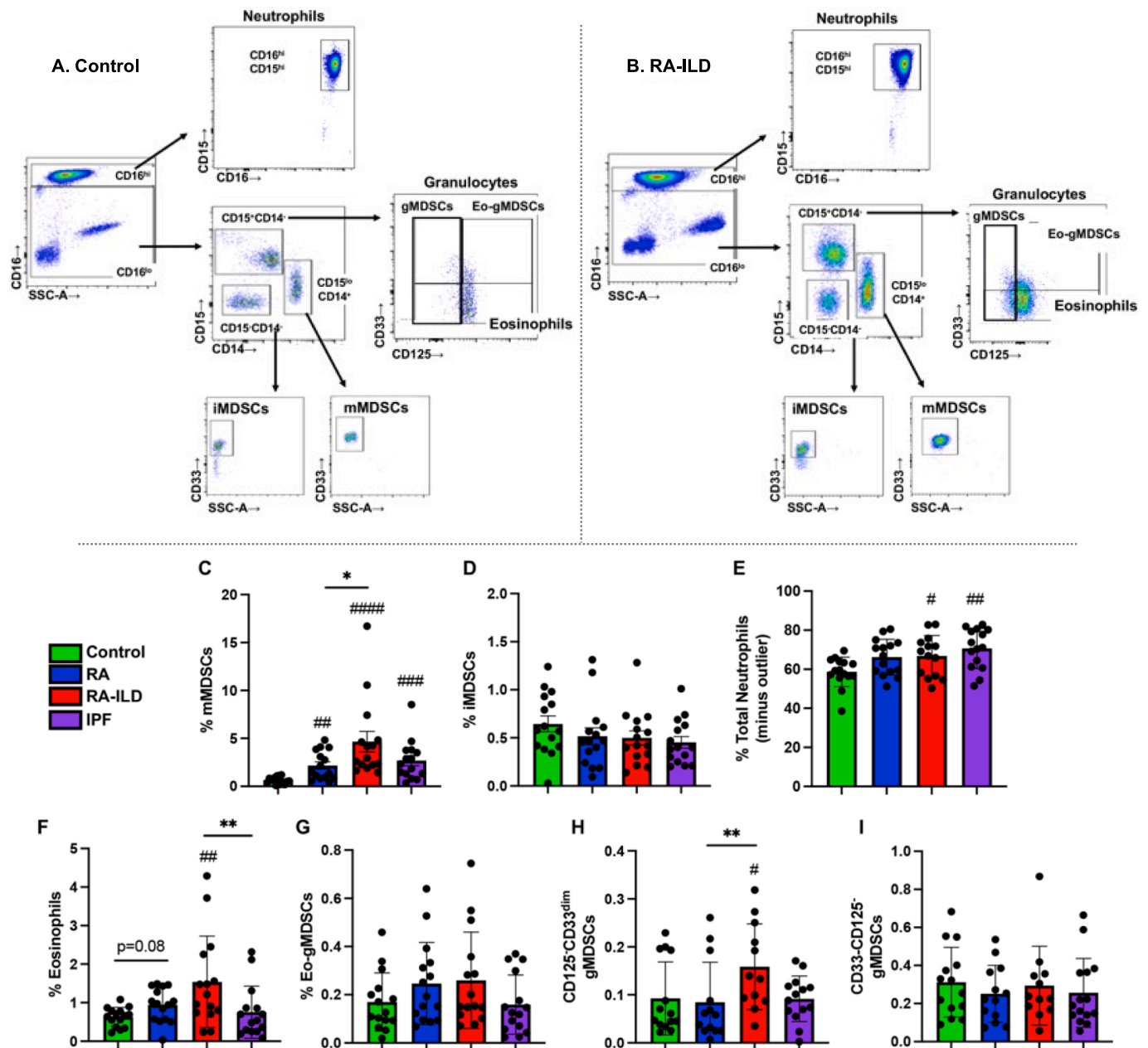
Fig. 2. Peripheral blood myeloid derived suppressor cells (MDSCs), neutrophils and eosinophils across groups. Representative contour plots from a control (**A**) and RA-ILD (**B**) showing live CD45$^+$CD11b$^+$HLA-DR^{lo} cells (Fig. 1) gated on CD16 high vs. low expression with subpopulations gated on CD15, CD14, CD33, and CD125 (IL-5Rα). Scatter plots of mean with SEM of percent (%) population of CD45$^+$ cells (**C-I**). Subpopulations of monocytic (m)MDSCs (**C**, CD16^{lo}CD15^{lo}CD14$^+$CD33$^+$), immature (i)MDSCs (**D**, CD16^{lo}CD15$^-$CD14$^-$CD33$^+$), neutrophils (**E**, minus 1 RA-ILD outlier with extreme neutropenia, CD16^{hi}CD15^{hi}), eosinophils (Eo) (**F**, CD16^{lo}CD15$^+$CD14$^-$CD125$^+$CD33$^-$), Eo-granulocytic (g)MDSCs (**G**, CD16^{lo}CD15$^+$CD14$^-$CD125$^+$CD33^{dim}), CD125$^-$CD33^{dim} gMDSCs (**H**, CD16^{lo}CD15$^+$CD14$^-$CD125$^-$CD33$^{dim/-}$), and CD125$^-$CD33$^-$ gMDSCs (**I**, CD16^{lo}CD15$^+$CD14$^-$CD125$^-$CD33$^-$). Statistical difference (##p < 0.01, ###p < 0.001, ####p < 0.0001) versus control and between groups (*p < 0.05).

3.5. Summary of frequency, fold-differences and absolute numbers of all cell subpopulations

Collectively, the frequency of these myeloid cell subpopulations is summarized in **Supplemental Table 2**. Of note, the frequency of total LIN$^+$ cells (CD3$^+$ T cells, CD19$^+$ B cells and CD56$^+$ NK cells) was decreased in RA, RA-ILD, and IPF vs. controls. The fold-change vs. control (referent group) in absolute numbers across groups is depicted in Table 2. We note approximately a 1.5- to 3-fold increase in absolute number of monocytes, eosinophils, Eo-g-MDSCs and neutrophils and an 8-fold increase in mMDSCs in the RA-ILD patients vs. controls (Table 2). Overall, the total number of leukocytes was significantly increased in RA

and IPF and trended for RA-ILD (p = 0.08) vs. control (Table 3). The frequency of the cell subpopulations relative to CD45$^+$ cells were then multiplied by total leukocytes to demonstrate increase absolute numbers of all myeloid cell subpopulations (except iMDSCs and CD33$^-$CD125$^-$ gMDSCs) (Table 3).

3.6. Frequency and absolute cellular numbers of intracellular iNOS expression across monocyte subpopulations and mMDSCs

Herein, we report on both iNOS expression (MFI and % expression) of classical, intermediate, non-classical monocytes and mMDSCs within each patient group (Fig. 3**A–B**) and absolute numbers of iNOS$^+$

Table 2
Peripheral blood leukocyte subpopulation numbers represented as fold-change vs. control (referent group).

Cell population	Controls (Referent)	RA	RA-ILD	IPF
Total Leukocytes	1.0	**1.4#**	1.3	**1.7##**
LIN+ Lymphocytes	1.0	1.0	0.9	1.1
HLA-DR+ Monocytes	1.0	**1.7##**	**1.5#**	**1.9####**
-Classical Monocytes	1.0	**1.1##**	**0.6#, *, †**	1.2
-Intermediate Monocytes	1.0	**2.0#**	**1.9#**	**2.4###**
–Non-Classical Monocytes	1.0	**2.1#**	**2.3#,†**	**2.8####**
Neutrophils	1.0	**1.6#**	**1.5#**	**2.0###**
Eosinophils	1.0	**1.7#**	**3.0###**	2.3
mMDSCs	1.0	**5.0##**	**7.7####**	**6.7###**
iMDSCs	1.0	1.1	1.0	1.3
Eo-gMDSCs	1.0	**2.1#**	**2.1#**	2.0
CD33dimCD125- gMDSCs	1.0	1.0	**1.8##, ***	1.4
CD33-CD125- gMDSCs	1.0	1.1	1.8	1.5

LIN (CD3+, CD19+, CD56+, lymphocytes). Immature (i), monocytic (m), granulocytic (g), eosinophilic (Eo). N = 15/group except for gMDSCs (N = 12–14/group) and RA-ILD neutrophil (N = 14).
Significance in bold, # significant vs. control patients (#p < 0.05, ##p < 0.01, ###p < 0.001, ####p < 0.0001). * significant vs. RA (*p < 0.05, **p < 0.01, ***p < 0.001), † significant vs. IPF (†p < 0.05).

Table 3
Absolute numbers of peripheral blood leukocyte subpopulations.

Cell population	Controls	RA	RA-ILD	IPF
Total Leukocytes, x10^6	4.7 ± 0.4	**6.6 ± 0.6#**	6.1 ± 0.5	**7.9 ± 0.7##**
LIN+ Lymphocytes, x10^6	1.3 ± 0.1	1.3 ± 0.1	1.2 ± 0.1	1.4 ± 0.2
HLA-DR+ Monocytes, x10^5	2.9 ± 0.3	**4.8 ± 0.5##**	**4.4 ± 0.3#**	**5.4 ± 0.5####**
-Classical Monocytes, x10^5	2.1 ± 0.3	**2.4 ± 0.3##**	**1.3 ± 0.2#, *,†**	2.6 ± 0.4
-Intermediate Monocytes, x10^4	2.7 ± 0.3	**5.5 ± 1.1#**	**5.1 ± 0.7##**	**6.6 ± 1.0###**
–Non-Classical Monocytes, x10^4	1.7 ± 0.2	**3.5 ± 0.6##**	**3.9 ± 0.9#,†**	**4.8 ± 0.6####**
Neutrophils, x10^6	2.8 ± 0.3	**4.5 ± 0.6#**	**4.2 ± 0.5#**	**5.7 ± 0.6###**
Eosinophils, x10^5	0.3 ± 0.1	**0.5 ± 0.1#**	**0.9 ± 0.1###**	0.7 ± 0.2
mMDSCs, x10^5	0.3 ± 0.1	**1.5 ± 0.3##**	**2.3 ± 0.3####**	**2.0 ± 0.3###**
iMDSCs, x10^4	2.8 ± 0.4	3.2 ± 0.5	2.9 ± 0.5	3.7 ± 0.6
Eo-gMDSCs, x10^4	0.7 ± 0.1	**1.5 ± 0.3#**	**1.5 ± 0.3#**	1.4 ± 0.3
CD33dimCD125- gMDSCs, x10^4	0.5 ± 0.1	0.5 ± 0.1	**0.9 ± 0.1##,***	0.7 ± 0.1
CD33-CD125- gMDSCs, x10^4	1.5 ± 0.3	1.7 ± 0.3	2.7 ± 0.9	2.2 ± 0.5

Mean ± SEM as determined by total cells per mL. Total leukocytes multiplied by % cell subpopulation as a proportion of CD45+ cells.
LIN (CD3+, CD19+, CD56+), immature (i), monocytic (m), granulocytic (g), eosinophilic (Eo). N = 15/group except for gMDSCs (N = 12–14/group) and RA-ILD neutrophil (N = 14).
Significance in bold, # significant vs. control patients (#p < 0.05, ##p < 0.01, ###p < 0.001, ####p < 0.0001). * significant vs. RA (*p < 0.05, **p < 0.01, ***p < 0.001), † significant vs. IPF (†p < 0.05).

monocyte subpopulations and mMDSCs (Table 4). Within controls, RA, and IPF, there was a pattern of reductions in iNOS expression with intermediate and non-classical monocytes but increased iNOS expression with mMDSCs vs. classical monocytes. This pattern of reduced iNOS expression with intermediate and non-classical monocytes was lost among RA-ILD patients but iNOS remained elevated in RA-ILD mMDSCs vs. classical monocytes. In comparing iNOS expression across groups for each subpopulation, IPF demonstrated increased iNOS expression for all

monocyte subpopulations vs. controls. There was no difference in iNOS expression for iMDSCs across subject groups (data not shown) with low mean iNOS expression by MFI (controls: 26, RA: 31, RA-ILD: 38 IPF: 42). Intracellular Arg-1 expression did not differ among monocyte subpopulations, mMDSCs, and iMDSCs or between participant groups (data not shown). The numbers of iNOS+ intermediate monocytes as well as mMDSCs were increased in RA, RA-ILD, and IPF vs. control subjects, which in part reflects the increased number of these monocyte subsets. Moreover, numbers of iNOS+ classical monocytes and iNOS+ non-classical monocytes were increased in IPF patients vs. controls.

3.7. Frequency and absolute cellular numbers of intracellular Arg-1 and iNOS expression across granulocyte populations and precursors

Intracellular Arg-1 MFI expression was increased in neutrophils of patients with IPF (+97 %,) vs. control with trends observed for RA-ILD (+52 %, p = 0.06) but not RA (Fig. 3C). The absolute numbers of Arg-1+ neutrophils were increased in RA, RA-ILD, and IPF patients vs. controls, and in IPF patients, there were significantly increased Arg-1+ neutrophils as compared to RA and RA-ILD (Table 4). Conversely, iNOS expression in neutrophils was high with no difference in MFI expression across groups (Fig. 3D). However, the absolute numbers of iNOS+ neutrophils were increased in RA, RA-ILD, and IPF patients vs. controls (Table 4). For eosinophils, Arg-1 expression was low with no difference across groups, but the absolute Arg-1+ eosinophil numbers were increased in patients with RA and RA-ILD vs. both controls and IPF patients (Table 4). Whereas iNOS expression was increased in both RA (+46 %) vs. control, there was wide variability in iNOS expression in RA-ILD participants. However, the absolute number of iNOS+ eosinophils were increased in RA and RA-ILD (but not IPF) vs. control subjects. Correspondingly, iNOS expression was significantly increased in Eo-gMDSCs of RA subjects vs. control (+143 %), RA-ILD (+15 %), and IPF (+59 %) with Arg-1 also increased in RA (+66 %) vs. IPF. Moreover, absolute numbers of iNOS+ Eo-gMDSCs were increased in patients with RA and RA-ILD (but not IPF) vs. controls, and Arg-1+ Eo-gMDSCs were also increased in RA and RA-ILD vs both IPF and controls (Table 4). For CD33dimCD125- gMDSCs, Arg-1 expression was decreased in IPF vs. RA (–33 %) and RA-ILD (-34 %) but not control, and iNOS expression was decreased in IPF (-29 %) vs. control. Correspondingly, absolute numbers of both iNOS+ and Arg-1+ CD33dimCD125- gMDSCs were increased only with RA-ILD patients (Table 4). There was no difference between the groups for iNOS expression and absolute numbers of CD33-CD125- gMDSCs. Whereas there was no difference in Arg-1 expression of CD33-CD125- gMDSCs, absolute numbers of these cell were increased in RA and RA-ILD vs. IPF.

3.8. Clustering of CD45+ cells

To provide visualization of the complex multi-dimensional data, the tSNE algorithm was applied to CD45+ cells combined from a representative subject from each group including from each of the three RA-ILD lung CT imaging categories (Fig. 4A-C). The embedded tSNE mapping of the data is demonstrated by contour plot with overlay colors (and shape outlines) labeling subpopulations by described gating strategies with representative groups subsequently separated from the combined map to provide visualization of the cellular distribution differences across groups. Neutrophils represent the largest cluster, with high Arg-1 expression distinguishing shared neutrophil dimensions for Category 1 RA-ILD (UIP, fibrosis) and IPF (Fig. 4A), consistent with flow analysis (Fig. 3C–D). The monocytes and mMDSCs cluster within close dimensions that vary across groups. The lymphocytes (LIN+ cells) are further delineated by HLA-DR expression noting that B cells typically express HLA-DR. The eosinophil cluster demonstrates slight dimensional shifts with RA-ILD vs. all other groups. Due to low frequency, the remainder of the MDSCs and otherwise undifferentiated cells do not differ remarkably.
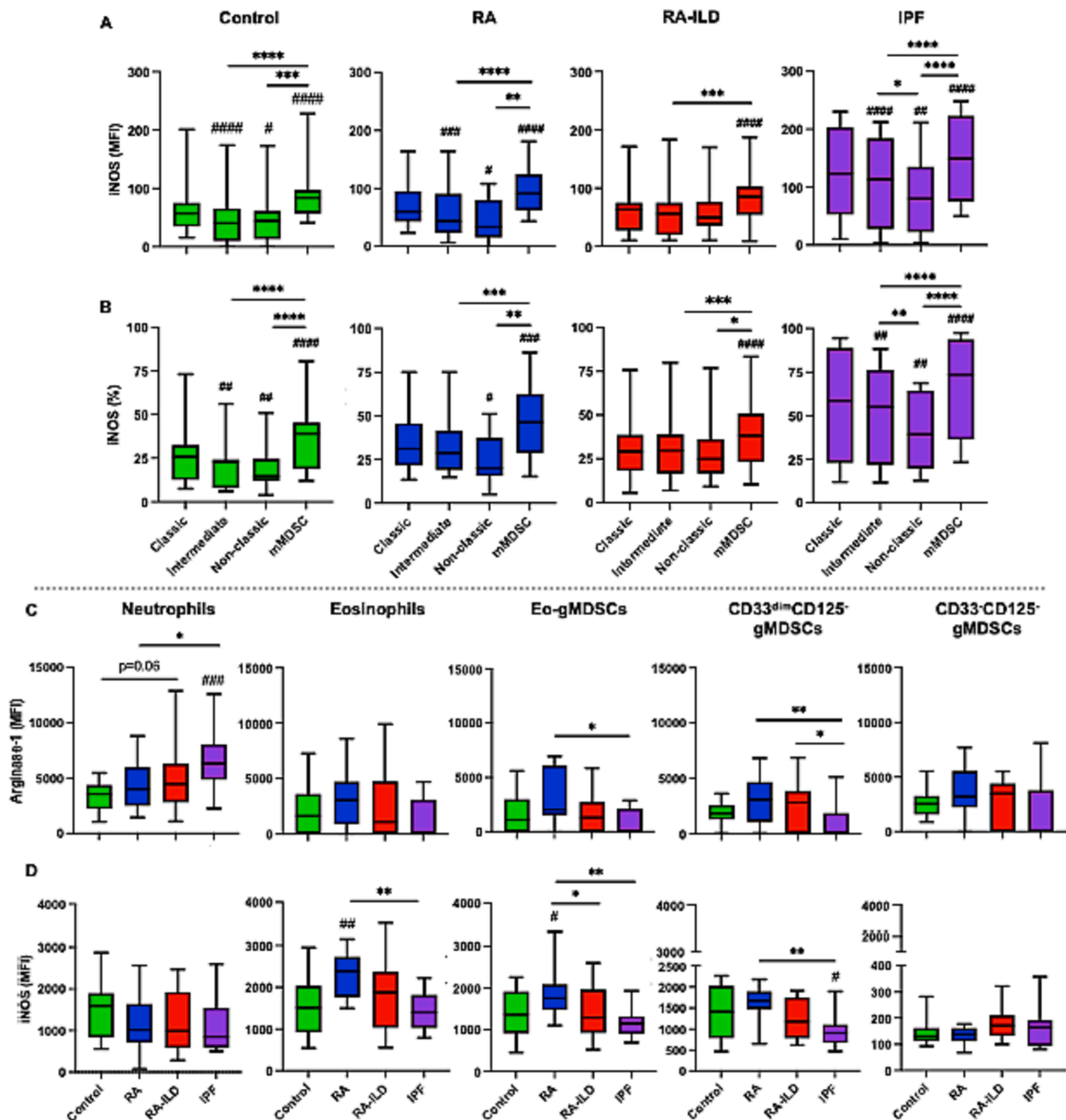
Fig. 3. Pattern of intracellular iNOS and Arg-1 expression across peripheral blood myeloid cell subpopulations. Box and whisker (min to max) graphs of intracellular staining for inducible nitric oxide synthase (iNOS) represented as mean fluorescent intensity (MFI, **A**) and percent expression (**B**) by subject-matched classical, intermediate, and non-classical monocytes and monocyte-myeloid derived suppressor cells (mMDSCs) per subject group. N = 15 (control, RA-ILD, IPF) and N = 14 (RA). Intracellular staining of Arg-1 (**C**) and iNOS (**D**) represented as MFI by subject group by granulocyte subpopulation. N = 12–15/group. Statistical difference (#p < 0.05, ##p < 0.01, ###p < 0.001, ####p < 0.0001) vs. controls and between groups denoted (*p < 0.05, **p < 0.01, ***p < 0.001, ****p < 0.0001).

4. Discussion

ILD remains the most overrepresented cause of death in RA [39–41]. Knowledge of critical cellular players, biomarkers of disease, and efficacious therapeutic options are limited. Increased peripheral blood monocytes and neutrophils are associated with poor outcomes in RA-ILD [17], and studies herein also demonstrated increased numbers of total monocytes and neutrophils in RA-ILD. However, there is little to no information about myeloid cell subsets in RA-ILD. Our studies rigorously analyzed total human peripheral blood leukocyte populations using

multiparametric flow panel to differentiate circulating monocyte subsets, neutrophils, eosinophils, and MDSC subsets of RA-ILD patients as compared to patients with RA without lung disease, IPF without autoimmunity, and control participants without any systemic, autoimmunity or lung disease. Collectively, there was a striking expansion of several distinct myeloid cell subpopulations in RA-ILD that shared more overlapping features with IPF than RA. This was illustrated quite strikingly using tSNE clustering approach, specifically for RA-ILD with a UIP-pattern or UIP-like features. In addition to IPF overlap, we identified myeloid cell subpopulations unique to RA-ILD including marked relative

Table 4
Absolute numbers of iNOS+ and Arg-1+ cell subpopulations.

Cell population	Controls	RA	RA-ILD	IPF
iNOS± Cell subpopulations				
Classical Monocytes, x10^5	0.63 ± 0.15	0.89 ± 0.21	0.45 ± 0.10	**1.57 ± 0.38** [##,$]
Intermediate Monocytes, x10^4	0.61 ± 0.20	**1.63 ± 0.30** [##]	**1.67 ± 0.5** [#]	**3.77 ± 0.88** [###]
Non-Classic Monocytes, x10^4	0.38 ± 0.11	0.9 ± 0.17	0.93 ± 0.24	**1.98 ± 0.43** [###,**]
Neutrophils, x10^6	2.67 ± 0.27	**4.3 ± 0.58** [#]	**4.05 ± 0.45** [#]	**5.45 ± 0.62** [##]
Eosinophils, x10^5	0.29 ± 0.04	**0.53 ± 0.06** [#]	**0.75 ± 0.15** [##]	0.66 ± 0.20
mMDSCs, x10^4	1.09 ± 0.32	**7.61 ± 2.37** [#]	**10.75 ± 2.53** [###]	**11.09 ± 1.82** [###]
iMDSCs, x10^4	0.19 ± 0.05	0.41 ± 0.08	0.41 ± 0.13	**0.72 ± 0.25** [##]
Eo-gMDSCs, x10^4	0.74 ± 0.15	**1.59 ± 0.29** [#]	**1.61 ± 0.30** [#]	1.31 ± 0.34
CD33dim CD125- gMDSCs, x10^4	0.42 ± 0.10	0.54 ± 0.15	**0.90 ± 0.12** [#,*]	0.67 ± 0.11
CD33- CD125- gMDSCs, x10^4	1.56 ± 0.29	1.74 ± 0.34	2.66 ± 0.88	2.07 ± 0.43
Arg-1± Cell subpopulations				
Neutrophils, x10^6	1.39 ± 0.23	**3.04 ± 0.59** [#]	**2.78 ± 0.48** [#]	**5.14 ± 0.57** [###,*,$]
Eosinophils, x10^5	0.07 ± 0.03	**0.27 ± 0.07** [#,††]	**0.46 ± 0.17** [#,††]	0.47 ± 0.02
Eo-gMDSCs, x10^4	0.05 ± 0.02	**0.43 ± 0.11** [##,††]	**0.59 ± 0.17** [##,††]	0.10 ± 0.05
CD33dim CD125- gMDSCs, x10^4	0.07 ± 0.03	0.22 ± 0.09	**0.50 ± 0.12** [##,††]	0.09 ± 0.03
CD33- CD125- gMDSCs, x10^4	0.41 ± 0.11	**0.93 ± 0.30** [††]	**1.0 ± 0.28** [††]	0.32 ± 0.17

Mean ± SEM as determined by total cells per mL. Total leukocytes multiplied by % cell subpopulation as a proportion of CD45+ cells.
immature (i), monocytic (m), granulocytic (g), eosinophilic (Eo). N = 15/group except for gMDSCs (N = 12–14/group) and RA-ILD neutrophil (N = 14). Significance in bold, # significant vs. control patients (#p < 0.05, ##p < 0.01, ###p < 0.001, ####p < 0.0001). * significant vs. RA (*p < 0.05, **p < 0.01, ***p < 0.001), † significant vs. IPF (†p < 0.05), $ significant vs. RA-ILD ($$p < 0.05, $$p < 0.01).

increase in eosinophils and slight increase in gMDSCs. Whether the overlap observed in circulating cell populations from patients with RA-ILD in a UIP pattern (the most frequent pattern in RA-ILD) and IPF reflects their common histopathologic/historadiologic characteristics or underlying shared genetic and environmental risk factors is unknown.

Dysregulation and expansion of intermediate and nonclassical monocytes in patients with RA has been previously reported [12–14] and confirmed in this study. Previous work has demonstrated that higher frequencies of CD16+ monocytes are associated with heightened articular disease activity in RA in addition to reduced treatment response to disease-modifying anti-rheumatic drugs (DMARDs) [14,42]. Although the relationship of these monocyte subsets with anti-citrullinated protein antibodies (ACPA) positivity has not been fully defined, a report found a frequency shift from classical monocytes to intermediate/non-classical monocytes in ACPA+ individuals at risk for the development of RA [12]. ACPA-containing immune complexes can activate FcR-positive cells resulting in proinflammatory mediator release [43,44]. As intermediate and nonclassical monocytes express CD16 (FcγRIII), RA disease activity may be increased in ACPA+ individuals with increased CD16+ expressing monocytes [12]. However, ACPA differences between groups in our study do not appear to explain these differences as more RA patients were ACPA+ (86.7 %) than RA-ILD (66.7 %). Thus, intermediate and non-classical monocytes may represent a more inflammatory monocyte subpopulation to herald RA disease activity via a potential pathogenic role. Consistent with this proposed

worsening disease phenotype, RA-ILD patients in our study had an increased frequency (and numbers) of intermediate monocytes as compared to RA, representing the majority of monocyte subsets in 47 % of the RA-ILD patients.

Although increased numbers of monocytes are also associated with poor prognosis in IPF [15,16], less has been described about the role of intermediate/non-classical monocytes in human IPF. One study reported that blood monocytes from patients with IPF display increased CD64 (FcγR1) expression, a marker of inflammatory monocyte-macrophages [45], with amplified type I interferon responses [46]. Our studies provide new support for the expansion of intermediate and non-classical monocytes in IPF at a similar magnitude as observed in RA-ILD patients. In addition, intermediate/nonclassical monocytes could potentially be targeted by anti-FcγR antibody immunotherapies that are under investigation in other chronic diseases [45].

MDSCs are recognized for their ability to suppress T cell number and function with mMDSCs recognized as a "more immunosuppressive" subpopulation in patients with autoimmune diseases [47]. A role for gMDSCs have been emphasized in studies of cancer prognosis and in murine models of autoimmunity [10,19,47,48]. In our studies, the frequency and numbers of mMDSCs were significantly increased in RA, RA-ILD and IPF with the frequency of mMDSCs higher in RA-ILD vs. RA patients. In other reports, MDSCs were demonstrated to inversely correlate with lung vital capacity in IPF but not in chronic obstructive pulmonary disease [49] or non-IPF ILD [22]. iNOS is a functional mediator of both monocytes and mMDSCs with immunosuppressive characteristics on T cell activity including suppression of regulatory T cells [20], and it also associated with inflammatory monocytes [26]. In our side-by-side comparison studies, iNOS expression was reduced in intermediate and non-classic monocytes (vs. classic monocytes) with the highest expression in mMDSCs. Of note, the absolute number of iNOS expressing mMDSCs were increased across RA, RA-ILD, and IPF subjects. The increase in number of iNOS intermediate monocytes across subpopulations reflects the overall increase in intermediate monocytes in diseased patients. The IPF patients in our study had the highest frequency of iNOS expression on all monocyte subsets and in mMDSCs, suggesting an enhanced immunosuppressive phenotype in these patients. Recognizing and better understanding the complexity of monocytic subpopulations could support a pathogenic role of the cellular inflammatory/immunosuppressive imbalance of RA-ILD.

Granulocytes including neutrophils and eosinophils are important immune effector cells with increased neutrophil numbers associated with poor prognosis in RA-ILD [17]. In our studies, the percentage (after removing single RA-ILD outlier) and number of neutrophils were increased in both RA-ILD and IPF. Neutrophil Arg-1 expression was elevated in IPF with similar trends in RA-ILD (p = 0.06), an observation supported by clustering (tSNE) analysis, demonstrating that neutrophil populations of RA-ILD (category 1, UIP) and IPF cluster in similar dimensions and are associated with high Arg-1 expression. This clustering analysis suggests that the peripheral blood cellular and functional immunophenotype of RA-ILD marked by UIP features shares strong similarities to that of non-autoimmune IPF (UIP pattern) as opposed to RA, suggests a potential conversion to a lung disease-driven systemic inflammatory response as opposed to arthritis-driven response. Future longitudinal studies are necessary to determine whether these peripheral blood immunophenotype signatures (or cellular biomarkers) predict risk of RA-ILD development in patients with RA. Human Arg-1 is constitutively expressed in granulocyte granules and liberated during inflammation and associated with their lymphocyte suppressive characteristics [20,50]. We also detected a slight, but significant increase in the frequency and numbers of gMDSCs in RA-ILD, and moreover, the absolute number of iNOS+ and Arg-1+ gMDSCs were also increased only in RA-ILD patients. Importantly, we identified another novel gating strategy that has not been previously undertaken in human MDSC studies but has been reported in murine studies [51]. Specifically, eosinophils were gated using CD125 (IL-5Rα) in two subpopulations of
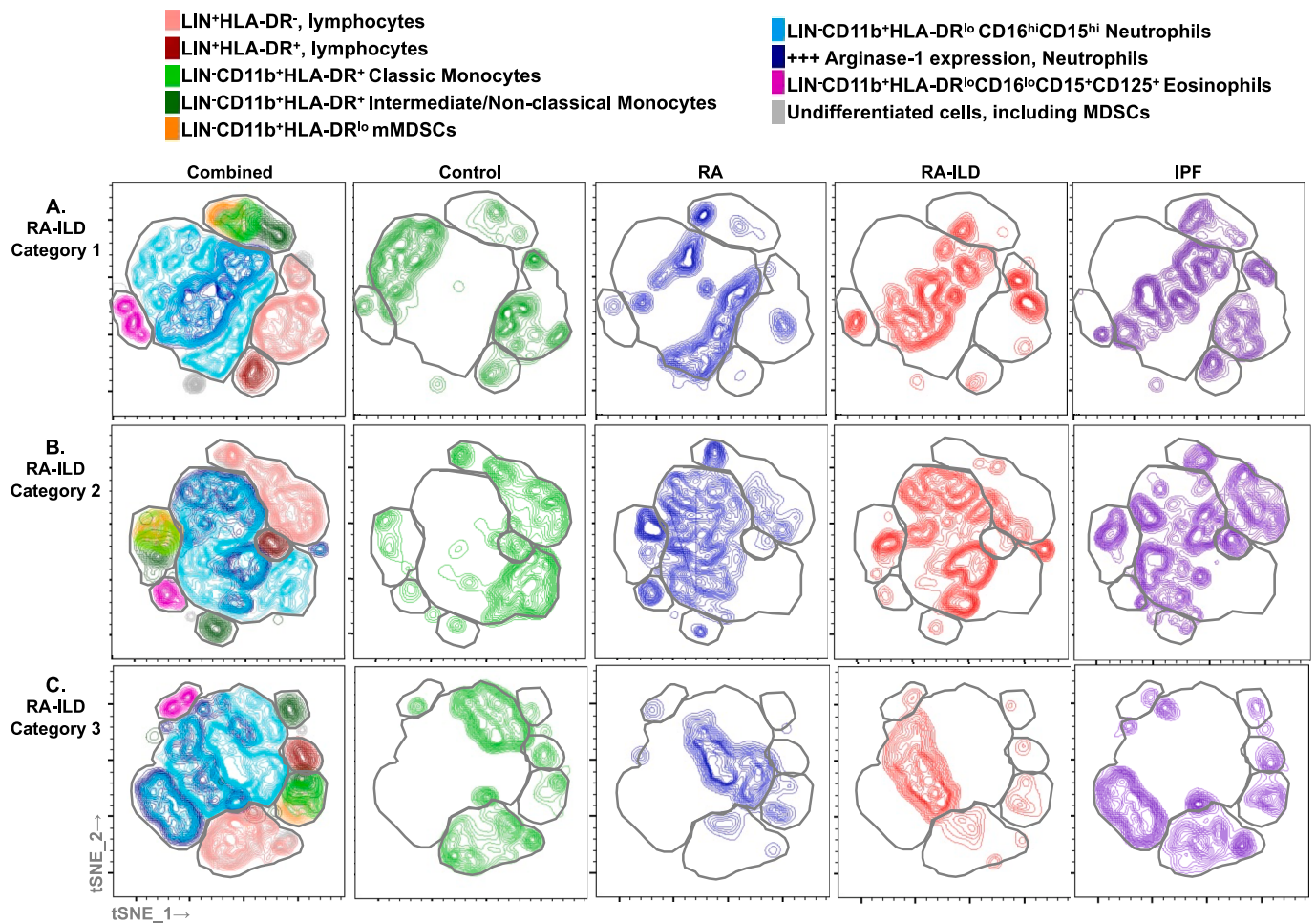
Fig. 4. Clustering by tSNE algorithm of a representative subject from each participant group. tSNE mapping of the data applied to CD45$^+$ cells combined of a representative subject from each group (control, RA, RA-ILD) by representative RA-ILD characterized as Category 1 (usual interstitial pneumonia, honeycombing or fibrosis, **A**), Category 2 (ground glass opacities, **B**), and Category 3 (other/indeterminate: subpleural reticulation, interstitial thickening, or reticular opacities, **C**) are demonstrated by contour plots and overlay colors (top panel)(and shape outlines) broadly labeling lymphoid and myeloid cell subpopulations (**left column**) with subsequent columns depicting plots of each group separated from the combined map with colors scheme consistent for each group (Control: green, RA: blue, RA-ILD: red, IPF: purple). (For interpretation of the references to colour in this figure legend, the reader is referred to the web version of this article.)

mature (CD33$^-$) and immature (CD33$^+$) cells, with the latter suggesting a gMDSC subset, an observation that warrants future investigation.

Whereas observations of eosinophilia in RA dates to the 1970′s [52], a pathogenic role for eosinophils in RA remains unclear. Thus, an unexpected finding from our study was the significant increase frequency in eosinophils in RA-ILD with a trend for an increase in RA patients. Furthermore, Eo-gMDSC numbers were increased in both RA and RA-ILD patients. Correspondingly, the absolute numbers of iNOS$^+$ and Arg-1$^+$ expressing eosinophils and Eo-gMDSCs (eosinophil precursors) were increased in RA and RA-ILD (but not IPF) patients. Although there is a paucity of data, eosinophilic lung infiltration in histologic patterns of RA-ILD has been previous acknowledged [53]. Serum levels of the eosinophil chemoattractant eotaxin [54] but not IL-5 [55] have been also associated with RA-ILD in single studies. Collectively, these observations of increased eosinophils and eosinophil precursors may be clinically important as eosinophil targeted immunotherapies have received regulatory approval for pulmonary diseases including asthma [24] and are emerging for COPD [25]. Thus, future studies exploring blood levels of eosinophils and eosinophil precursors may lead to an eosinophilic sub-phenotype of RA-ILD to guide more personalized approaches to disease management.

There are limitations to this study. The comparator controls were not age-matched to the diseased groups, and all had allergic rhinitis on specific therapy, which could impact circulating myeloid cell subpopulations. Moreover, we did not systematically rule out the possibility of subclinical ILD via advanced imaging or pulmonary function testing in RA participants. The possibility that these participants could have harbored subclinical lung disease is underscored by dyspnea symptoms scores approaching that of RA-ILD patients to suggest that differences observed between the RA-ILD and RA may represent conservative estimates. RA and RA-ILD patients were older and male predominant, which may limit the generalizability. Our sample size number was limited preventing subgroup analyses based on characteristics such as age, sex, articular disease activity, autoantibody positivity, DMARD receipt, or environmental factors such as cigarette smoking. Moreover, interpretation of non-UIP RA-ILD trends is limited by patient number.

In conclusion, patients with RA-ILD demonstrated increased numbers and frequency of monocytes, particularly intermediate and non-classical CD16$^+$ monocytes, mMDSCs, neutrophils, and eosinophils. The immunophenotypes were distinct from that of RA alone. Whereas the myeloid cell phenotype of RA-ILD shared many overlapping features with IPF, the increased eosinophil frequency was unique to RA-ILD. This knowledge of cellular immunophenotypes and function may also guide personalized approach to disease management, particularly related to monocyte subsets and eosinophil/eosinophil precursors. These studies justify a need for larger and longitudinal studies that will support an improved understanding of disease pathogenesis in RA-ILD and move us closer to a more personalized approach to disease management.

Disclosures.

JAP has received research regents (anti-IL-33/ST2 blocking antibody reagent, no monies) from AstraZeneca. JAP, JVDG, SMM, RW are site recruiters for clinical industry studies for asthma, sinus disease, and urticaria (GlaxoSmithKline, AstraZeneca, Regeneron Pharmaceuticals, CellDex Therapeutics). BRE has consulted with and received research support from Boehringer-Ingelheim. TRM has consulted for Horizon Therapeutics Pfizer, UCB, and Sanofi and receives research support from Horizon.

The views expressed in this article are those of the authors and do not necessarily reflect the position or policy of the Department of Veterans Affairs, the Department of Defense, or the United States government.

CRediT authorship contribution statement

Jill A. Poole: . **Kathryn E. Cole:** Data curation, Formal analysis, Investigation, Methodology, Validation, Visualization, Writing – review & editing, Writing – original draft. **Geoffrey M. Thiele:** . **James E. Talmadge:** Data curation, Formal analysis, Investigation, Methodology, Supervision, Visualization, Writing – original draft, Writing – review & editing. **Bryant R. England:** . **Amy J. Nelson:** Data curation, Investigation, Methodology, Writing – review & editing, Formal analysis, Visualization. **Angela Gleason:** Data curation, Investigation, Methodology, Writing – review & editing, Formal analysis, Visualization. **Aaron Schwab:** . **Rohit Gaurav:** . **Michael J. Duryee:** . **Kristina L. Bailey:** Data curation, Formal analysis, Investigation, Methodology, Visualization, Writing – review & editing. **Debra J. Romberger:** Data curation, Formal analysis, Investigation, Methodology, Visualization, Writing – review & editing. **Daniel Hershberger:** Data curation, Investigation, Methodology, Visualization, Writing – review & editing, Formal analysis. **Joel Van De Graaff:** Data curation, Formal analysis, Investigation, Methodology, Visualization, Writing – review & editing. **Sara M. May:** Data curation, Formal analysis, Investigation, Methodology, Visualization, Writing – review & editing. **Rhonda Walenz:** Data curation, Investigation, Methodology, Visualization, Writing – review & editing. **Bridget Kramer:** Data curation, Investigation, Methodology, Visualization, Writing – review & editing. **Ted R. Mikuls:** Conceptualization, Data curation, Formal analysis, Funding acquisition, Investigation, Methodology, Project administration, Resources, Software, Supervision, Validation, Visualization, Writing – original draft, Writing – review & editing.

Declaration of Competing Interest

The authors declare that they have no known competing financial interests or personal relationships that could have appeared to influence the work reported in this paper.

Data availability

Data will be made available on request.

Acknowledgements

Appendix A. Supplementary data

Supplementary data to this article can be found online at https://doi.org/10.1016/j.intimp.2023.111330.

References

[1] A.C. Duarte, J.C. Porter, M.J. Leandro, The lung in a cohort of rheumatoid arthritis patients-an overview of different types of involvement and treatment, Rheumatology (oxford). 58 (11) (2019) 2031–2038.
[2] D. Van Kalsbeek, R. Brooks, D. Shaver, A. Ebel, D. Hershberger, C. Schmidt, et al., Peripheral blood biomarkers for rheumatoid arthritis-associated interstitial lung disease: A systematic review, ACR Open Rheumatol. 5 (4) (2023) 201–226.
[3] S. Kadura, G. Raghu, Rheumatoid arthritis-interstitial lung disease: manifestations and current concepts in pathogenesis and management, Eur Respir Rev. 30 (160) (2021).
[4] B.R. England, D. Hershberger, Management issues in rheumatoid arthritis-associated interstitial lung disease, Curr Opin Rheumatol. 32 (3) (2020) 255–263.
[5] A. Manfredi, F. Luppi, G. Cassone, C. Vacchi, C. Salvarani, M. Sebastiani, Pathogenesis and treatment of idiopathic and rheumatoid arthritis-related interstitial pneumonia. The possible lesson from COVID-19 pneumonia, Expert Rev Clin Immunol. 16 (8) (2020) 751–770.
[6] R. Brooks, J.F. Baker, Y. Yang, P. Roul, G.S. Kerr, A.M. Reimold, et al., The impact of disease severity measures on survival in U.S. Veterans with rheumatoid arthritis-associated interstitial lung disease, Rheumatology (oxford). (2022).
[7] K. Raimundo, J.J. Solomon, A.L. Olson, A.M. Kong, A.L. Cole, A. Fischer, et al., Rheumatoid arthritis-interstitial lung disease in the United States: Prevalence, Incidence, and Healthcare Costs and Mortality, The Journal of Rheumatology. 46 (4) (2019) 360–369.
[8] M. Shaw, B.F. Collins, L.A. Ho, G. Raghu, Rheumatoid arthritis-associated lung disease, European Respiratory Review: An Official Journal of the European Respiratory Society. 24 (135) (2015) 1–16.
[9] D. Gilligan, C. O'Connor, K. Ward, D. Moloney, B. Bresnihan, M. FitzGerald, Bronchoalveolar lavage in patients with mild and severe rheumatoid lung disease, Thorax. 45 (8) (1990) 591–596.
[10] D. Wang, J. Zhang, J. Lau, S. Wang, V. Taneja, E.L. Matteson, et al., Mechanisms of lung disease development in rheumatoid arthritis, Nature Reviews Rheumatology. 15 (10) (2019) 581–596.
[11] J. Yang, L. Zhang, C. Yu, X.-F. Yang, H. Wang, Monocyte and macrophage differentiation: Circulation inflammatory monocyte as biomarker for inflammatory diseases, Biomarker Research. 2 (1) (2014) 1.
[12] K. Prajzlerova, O. Krystufkova, M. Komarc, H. Mann, H. Hulejova, N. Petrovska, et al., The dysregulation of monocyte subpopulations in individuals at risk of developing rheumatoid arthritis, Rheumatology (oxford). 60 (4) (2021) 1823–1831.
[13] M. Rossol, S. Kraus, M. Pierer, C. Baerwald, U. Wagner, The CD14(bright) CD16+ monocyte subset is expanded in rheumatoid arthritis and promotes expansion of the Th17 cell population, Arthritis Rheum. 64 (3) (2012) 671–677.
[14] N. Kawanaka, M. Yamamura, T. Aita, Y. Morita, A. Okamoto, M. Kawashima, et al., CD14+, CD16+ blood monocytes and joint inflammation in rheumatoid arthritis, Arthritis Rheum. 46 (10) (2002) 2578–2586.
[15] M.K.D. Scott, K. Quinn, Q. Li, R. Carroll, H. Warsinske, F. Vallania, et al., Increased monocyte count as a cellular biomarker for poor outcomes in fibrotic diseases: A retrospective, multicentre cohort study, Lancet Respir Med. 7 (6) (2019) 497–508.
[16] M. Kreuter, J.S. Lee, A. Tzouvelekis, J.M. Oldham, P.L. Molyneaux, D. Weycker, et al., Monocyte count as a prognostic biomarker in patients with idiopathic pulmonary fibrosis, Am J Respir Crit Care Med. 204 (1) (2021) 74–81.
[17] A. Saku, T. Fujisawa, K. Nishimoto, K. Yoshimura, H. Hozumi, M. Karayama, et al., Prognostic significance of peripheral blood monocyte and neutrophil counts in rheumatoid arthritis-associated interstitial lung disease, Respir Med. 182 (2021) 106420.
[18] S.M. Choi, Y. Mo, J.Y. Bang, Y.G. Ko, Y.H. Ahn, H.Y. Kim, et al., Classical monocyte-derived macrophages as therapeutic targets of umbilical cord mesenchymal stem cells: Comparison of intratracheal and intravenous administration in a mouse model of pulmonary fibrosis, Respir Res. 24 (1) (2023) 68.
[19] K. Cole, Z. Al-Kadhimi, J.E. Talmadge, Role of myeloid-derived suppressor cells in tumor recurrence, Cancer Metastasis Rev. 42 (1) (2023) 113–142.
[20] J.G. Navashenaq, A.G. Shabgah, M. Hedayati-Moghadam, N. Ariaee, H. Mohammadi, M. Hemmatzadeh, et al., The role of myeloid-derived suppressor cells in rheumatoid arthritis: An update, Life Sci. 269 (2021) 119083.
[21] T. Liu, F. Gonzalez De Los Santos, AE. Rinke, C. Fang, KR. Flaherty, SH. Phan, B7H3-dependent myeloid-derived suppressor cell recruitment and activation in pulmonary fibrosis, Front Immunol. 13 (2022) 901349.
[22] I.E. Fernandez, F.R. Greiffo, M. Frankenberger, J. Bandres, K. Heinzelmann, C. Neurohr, et al., Peripheral blood myeloid-derived suppressor cells reflect disease status in idiopathic pulmonary fibrosis, Eur Respir J. 48 (4) (2016) 1171–1183.

[23] P. Akuthota, H.B. Wang, L.A. Spencer, P.F. Weller, Immunoregulatory roles of eosinophils: a new look at a familiar cell, Clin Exp Allergy. 38 (8) (2008) 1254–1263.

[24] J.S. Bernstein, M.E. Wechsler, Eosinophilic respiratory disorders and the impact of biologics, Curr Opin Pulm Med. 29 (3) (2023) 202–208.

[25] M.G. Matera, L. Calzetta, M. Cazzola, J. Ora, P. Rogliani, Biologic therapies for chronic obstructive pulmonary disease, Expert Opin Biol Ther. 23 (2) (2023) 163–173.

[26] S. Kossmann, H. Hu, S. Steven, T. Schonfelder, D. Fraccarollo, Y. Mikhed, et al., Inflammatory monocytes determine endothelial nitric-oxide synthase uncoupling and nitro-oxidative stress induced by angiotensin II, J Biol Chem. 289 (40) (2014) 27540–27550.

[27] I.L.A.A. Marti, W. Reith, Arginine-dependent immune responses, Cell Mol Life Sci. 78 (13) (2021) 5303–5324.

[28] S.B. Abramson, A.R. Amin, R.M. Clancy, M. Attur, The role of nitric oxide in tissue destruction, Best Pract Res Clin Rheumatol. 15 (5) (2001) 831–845.

[29] F.C. Arnett, S.M. Edworthy, D.A. Bloch, D.J. McShane, J.F. Fries, N.S. Cooper, et al., The american rheumatism association 1987 revised criteria for the classification of rheumatoid arthritis, Arthritis Rheum. 31 (3) (1988) 315–324.

[30] V. Lenters, I. Basinas, L. Beane-Freeman, P. Boffetta, H. Checkoway, D. Coggon, et al., Endotoxin exposure and lung cancer risk: A systematic review and meta-analysis of the published literature on agriculture and cotton textile workers, Cancer Causes & Control : CCC. 21 (4) (2010) 523–555.

[31] J.T. Giles, S.K. Danoff, J. Sokolove, C.A. Wagner, R. Winchester, D.A. Pappas, et al., Association of fine specificity and repertoire expansion of anticitrullinated peptide antibodies with rheumatoid arthritis associated interstitial lung disease, Annals of the Rheumatic Diseases. 73 (8) (2014) 1487–1494.

[32] E.G. Eakin, P.M. Resnikoff, L.M. Prewitt, A.L. Ries, R.M. Kaplan, Validation of a new dyspnea measure: The UCSD shortness of breath questionnaire. University of California, San Diego Chest. 113 (3) (1998) 619–624.

[33] K.E. Cole, Q.P. Ly, M.A. Hollingsworth, J.L. Cox, J.C. Padussis, J.M. Foster, et al., Human splenic myeloid derived suppressor cells: Phenotypic and clustering analysis, Cell Immunol. 363 (2021) 104317.

[34] J.P. McCracken, G.A. Wellenius, G.S. Bloomfield, R.D. Brook, H.E. Tolunay, D. W. Dockery, et al., Household air pollution from solid fuel use: Evidence for links to CVD, Global Heart. 7 (3) (2012) 223–234.

[35] A.C. Thomas, J.T. Mattila, "Of mice and men": arginine metabolism in macrophages, Front Immunol. 5 (2014) 479.

[36] L. Maaten, G. Hinton, Visualizing data using t-SNE, Journal of Machine Learning Research 9 (2008) 2579–02605.

[37] S.A. Julious, Sample size of 12 per group rule of thumb for a pilot study, Pharmaceutical Statistics: The Journal of Applied Statistics in the Pharmaceutical Industry. 4 (4) (2005) 287–291.

[38] Y. Benjamini, D. Drai, G. Elmer, N. Kafkafi, I. Golani, Controlling the false discovery rate in behavior genetics research, Behavioural Brain Research. 125 (1–2) (2001) 279–284.

[39] C.A. Kelly, V. Saravanan, M. Nisar, S. Arthanari, F.A. Woodhead, A.N. Price-Forbes, et al., Rheumatoid arthritis-related interstitial lung disease: Associations, prognostic factors and physiological and radiological characteristics—A large multicentre UK study, Rheumatology. 53 (9) (2014) 1676–1682.

[40] B.R. England, H. Sayles, K. Michaud, G.M. Thiele, J.A. Poole, L. Caplan, et al., Chronic lung disease in U.S. Veterans with rheumatoid arthritis and the impact on survival, Clinical Rheumatology. 37 (11) (2018) 2907–2915.

[41] B.R. England, H. Sayles, K. Michaud, L. Caplan, L.A. Davis, G.W. Cannon, et al., Cause-specific mortality in male US veterans with rheumatoid arthritis, Arthritis Care & Research. 68 (1) (2016) 36–45.

[42] S. Wijngaarden, J.A. van Roon, J.G. van de Winkel, J.W. Bijlsma, F.P. Lafeber, Down-regulation of activating Fcgamma receptors on monocytes of patients with rheumatoid arthritis upon methotrexate treatment, Rheumatology (oxford). 44 (6) (2005) 729–734.

[43] L. Laurent, C. Clavel, O. Lemaire, F. Anquetil, M. Cornillet, L. Zabranecki, et al., Fcgamma receptor profile of monocytes and macrophages from rheumatoid arthritis patients and their response to immune complexes formed with autoantibodies to citrullinated proteins, Ann Rheum Dis. 70 (6) (2011) 1052–1059.

[44] C. Clavel, L. Nogueira, L. Laurent, C. Iobagiu, C. Vincent, M. Sebbag, et al., Induction of macrophage secretion of tumor necrosis factor alpha through Fcgamma receptor IIa engagement by rheumatoid arthritis-specific autoantibodies to citrullinated proteins complexed with fibrinogen, Arthritis Rheum. 58 (3) (2008) 678–688.

[45] O.A. Akinrinmade, S. Chetty, A.K. Daramola, M.U. Islam, T. Thepen, S. Barth, CD64: An attractive immunotherapeutic target for M1-type macrophage mediated chronic inflammatory diseases, Biomedicines. 5 (3) (2017).

[46] E. Fraser, L. Denney, A. Antanaviciute, K. Blirando, C. Vuppusetty, Y. Zheng, et al., Multi-modal characterization of monocytes in idiopathic pulmonary fibrosis reveals a primed type I interferon immune phenotype, Front Immunol. 12 (2021) 623430.

[47] G.F. van Wigcheren, D. Roelofs, C.G. Figdor, G. Florez-Grau, Three distinct tolerogenic CD14(+) myeloid cell types to actively manage autoimmune disease: Opportunities and challenges, J Autoimmun. 120 (2021) 102645.

[48] D. Lindau, P. Gielen, M. Kroesen, P. Wesseling, G.J. Adema, The immunosuppressive tumour network: Myeloid-derived suppressor cells, regulatory T cells and natural killer T cells, Immunology. 138 (2) (2013) 105–115.

[49] A. Agusti, L.D. Edwards, S.I. Rennard, W. MacNee, R. Tal-Singer, B.E. Miller, et al., Persistent systemic inflammation is associated with poor clinical outcomes in COPD: A novel phenotype, PloS One. 7 (5) (2012) e37483.

[50] M. Munder, F. Mollinedo, J. Calafat, J. Canchado, C. Gil-Lamaignere, J.M. Fuentes, et al., Arginase I is constitutively expressed in human granulocytes and participates in fungicidal activity, Blood. 105 (6) (2005) 2549–2556.

[51] S. Brandau, S. Trellakis, K. Bruderek, D. Schmaltz, G. Steller, M. Elian, et al., Myeloid-derived suppressor cells in the peripheral blood of cancer patients contain a subset of immature neutrophils with impaired migratory properties, J Leukoc Biol. 89 (2) (2011) 311–317.

[52] R.J. Winchester, D. Koffler, S.D. Litwin, H.G. Kunkel, Observations on the eosinophilia of certain patients with rheumatoid arthritis, Arthritis Rheum. 14 (5) (1971) 650–665.

[53] A. Picchianti Diamanti, V. Germano, E. Bizzi, B. Lagana, A. Migliore, Interstitial lung disease in rheumatoid arthritis in the era of biologics, Pulm Med. 2011 (2011) 931342.

[54] D.J. Kass, M. Nouraie, M.K. Glassberg, N. Ramreddy, K. Fernandez, L. Harlow, et al., Comparative profiling of serum protein biomarkers in rheumatoid arthritis-associated interstitial lung disease and idiopathic pulmonary fibrosis, Arthritis & Rheumatology. 72 (3) (2020) 409–419.

[55] N. Mena-Vazquez, F.J. Godoy-Navarrete, J.M. Lisbona-Montanez, R. Redondo-Rodriguez, S. Manrique-Arija, J. Rioja, et al., Inflammatory biomarkers in the diagnosis and prognosis of rheumatoid arthritis-associated interstitial lung disease, Int J Mol Sci. 24 (7) (2023).